**Supporting Information**

# Orientational Pair Correlations and Local Structure of Benzonitrile from Molecular Dynamics Simulations with Comparisons to Experiments

Maolin Sha[a, †, ‡], Steven A. Yamada[a, ‡], and Michael D. Fayer[*, ‡]

[†]Department of Physics and Materials Engineering
Hefei Normal University, Hefei 230061, China

[‡]Department of Chemistry
Stanford University, Stanford, CA 94305, USA
[*]Phone: (650) 723-4446; Email: fayer@stanford.edu

[a]Maolin Sha and Steven A. Yamada contributed equally to this work.

## 1. Modified OPLS-AA force field parameters for benzonitrile

All bond-angle parameters were directly used from the classic OPLS-AA force field. To build the mass center, M, into the topology, we redistributed the mass along the $C_M$-C≡N bond axis. Two atoms were used to describe the total mass of the $C_M$-C≡N bond axis, one is the mass center, M, and another is the ring carbon atom, $C_M$. Following the redistribution of mass, M has a mass of 24.1223 Da, and $C_M$ has a mass of 13.9058 Da. M is positioned at the center of mass of the C≡N bond. The distance between the $C_M$ and M atoms was set to 0.2212 nm as a constraint in the topology. The atoms in the C≡N bond were transformed into virtual atoms that no longer have mass but are able to interact with other atoms and molecules in the simulation. M has no interactions with other atoms. Note that the redistribution of masses leaves the moment of inertia of the benzonitrile molecule unchanged. The procedures for redistributing the atom masses and setting the atom positions can be found in Lemkul's Gromacs simulation tutorials.[1] The force field parameters are shown in Table S1.

**Table S1**. Lennard-Jones parameters, partial charges, and atomic masses for the modified OPLS-AA force field for benzonitrile.

| atom | $\sigma_{ij}$ (Å) | $\varepsilon_{ij}$ (kJ/mol) | $q$ (e) | mass (Da) |
|---|---|---|---|---|
| $C_H$ | 3.55 | 0.29288 | -0.115 | 12.0107 |
| H | 2.42 | 0.12552 | 0.115 | 1.0079 |
| C | 3.55 | 0.29288 | 0.050 | 0 |
| $C_M$ | 3.65 | 0.6276 | 0.450 | 13.9058 |
| M | 0 | 0 | 0 | 24.1223 |

| | | | | |
|---|---|---|---|---|
| N | 3.20 | 0.71128 | -0.500 | 0 |

## 2. Comparison of the dynamical properties of benzonitrile from our modified force field and other classic force fields

The thermodynamic and dynamical properties of benzonitrile can be calculated using the classic OPLS-AA force field.[2] We also calculated these properties of benzonitrile with the classic general Amber force field (GAFF)[3] and Charmm general force field (CGenFF).[4] All of these simulations were run for 10 ns in Gromacs with the same control parameters used in our modified OPLS-AA force field simulation. The last 2 ns were collected for analysis. These data are shown in Table 1 in the main text. In Fig. S1, we further compare an important benchmark dynamical property, the mean squared displacement (MSD), for benzonitrile using the modified OPLS-AA force field and the other three classic force fields. The details of the modified force field are discussed further in the main text and previous section, and the parameters are displayed in Table S1. The diffusion coefficient calculated using the modified force field is $(8.1 \pm 0.2) \times 10^{-6}$ $cm^2 \cdot s^{-1}$, which is closest to the experimental value estimated from the Stokes-Einstein (SE) equation (see below): $8.3 \times 10^{-6}$ $cm^2 \cdot s^{-1}$. Overall, the MSDs from OPLS-AA, our modified OPLS-AA, and Charmm are in good agreement with each other as shown in Fig. S1. The MSD from the generalized Amber force field is significantly steeper than the MSDs from the other force fields. This results in a diffusion coefficient ($1.2 \times 10^{-5}$ $cm^2 \cdot s^{-1}$) that is too large compared to the experimental value.

In comparison to these values, the translational diffusion coefficient of benzene at 298 K measured with the Carr-Purcell NMR spin echo method was determined to be $2.27 \times 10^{-5}$ $cm^2 \cdot s^{-1}$.[5] Also, the diffusion coefficient for pentafluorobenzonitrile ($C_6F_5CN$) was determined to be around $3.71 \times 10^{-6}$ $cm^2 \cdot s^{-1}$ at 298 K and 1 atm with $^{19}$F-NMR Fourier Transform Pulsed Gradient Spin Echos.[6] Both of these molecules are similar in size and structure to benzonitrile ($C_6H_5CN$) and are the most reasonable experimental benchmarks available in the literature. The diffusion coefficient we obtain using our modified force field is in reasonable agreement with the above experimental values, especially that for $C_6F_5CN$.

It is surprising that no translational diffusion coefficient for benzonitrile has been reported. However, many researchers have focused on viscosity measurements of neat benzonitrile and its mixtures with other solvents.[7-8] Since, to our knowledge, no diffusion coefficient has been reported for benzonitrile, we obtained it from the available viscosity data by

using the Stokes-Einstein equation. The SE equation is given by $D = k_B T / 6\pi\eta r$, where $k_B$ is the Boltzmann constant, $T$ is the absolute temperature, $\eta$ is the dynamic viscosity, and $r$ is the hydrodynamic radius. The hydrodynamic radius can be determined by calculating the van der Waals volume of the benzonitrile molecule. The van der Waals volume was calculated to be about 51 Å$^3$ with the Gaussian03 package.[9] Hence, the hydrodynamic radius of the molecule is about 2.3 Å. The experimental viscosity is 1.155 mPa·s.[7] Therefore, using the SE equation, the calculated value for the diffusion coefficient is $8.3 \times 10^{-6}$ cm$^2$·s$^{-1}$. The diffusion coefficient we calculate using the modified OPLS-AA force field is in quantitative agreement with the value obtained from the SE equation.

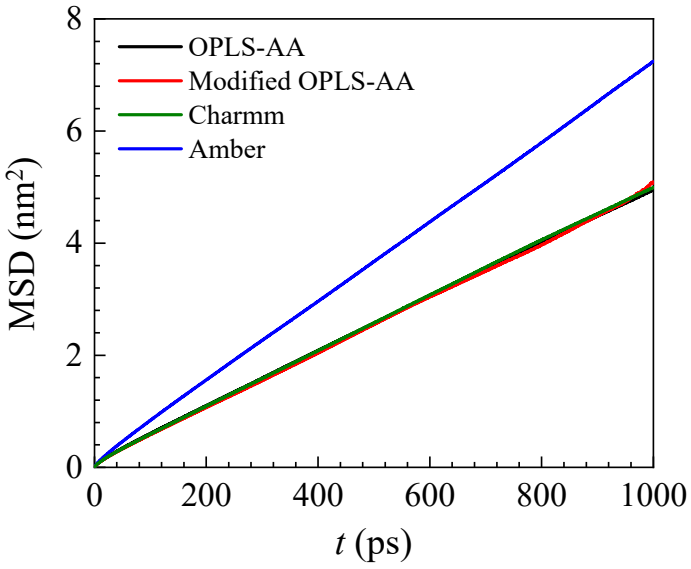


**Figure S1.** Mean squared displacement (MSD) of benzonitrile using our modified OPLS-AA force field and other classic force fields.

In addition to the MSD, we also calculated the orientational correlation function, $C_2(t)$, for the C-N bond vector of benzonitrile using our modified OPLS-AA force field and the classic force fields, introduced above, in Fig. S2. The trends are similar to the MSD, the Amber force field produces faster reorientation than the other force fields, while the remaining force fields are in good agreement. As shown in the main text, the anisotropy, $r(t) = 0.4C_2(t)$, from the modified OPLS-AA force field is in quantitative agreement with the experimentally measured anisotropy.

One needs to carefully use the generalized Amber force field to simulate the dynamics in liquid benzonitrile.

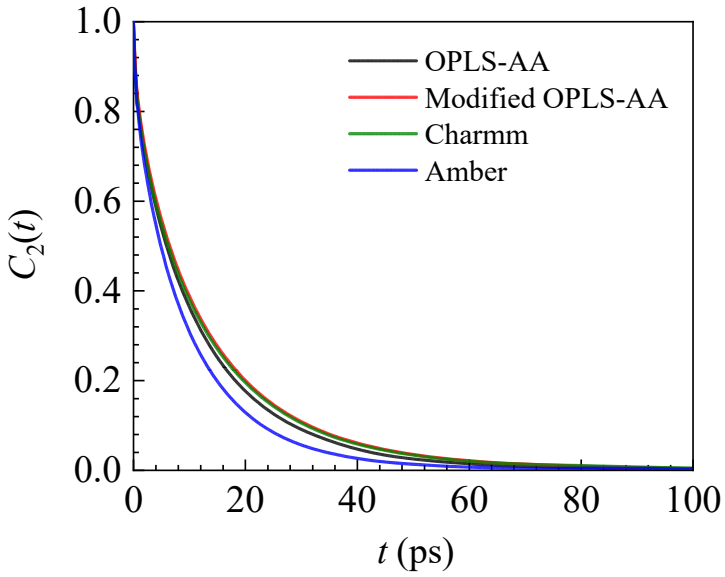


**Figure S2.** The orientational correlation functions, $C_2(t)$, for the C-N bond vector of benzonitrile using our modified OPLS-AA force field and other classic force fields.

The simulated OKE signals using the classic (blue curve) and modified (black curve) OPLS-AA force fields are compared to each other and to the measured OKE signal (red curve) in Fig. S3. The results from the two force fields are similar to each other; however, the modified force field obtains slightly better agreement with experiment particularly at intermediate and longer times. The polarizability anisotropy time correlation function (PA-TCF), in addition to its constituent molecular and interaction-induced auto-correlations and their cross-correlation, is shown in Fig. S4 for the classic and modified OPLS-AA force fields. Taken together, the comparisons indicate that the modified OPLS-AA force field provides the best agreement with the available experimentally measured properties of benzonitrile. Therefore, this force field was used to simulate the local intermolecular structures and dynamics in liquid benzonitrile presented in the main text.

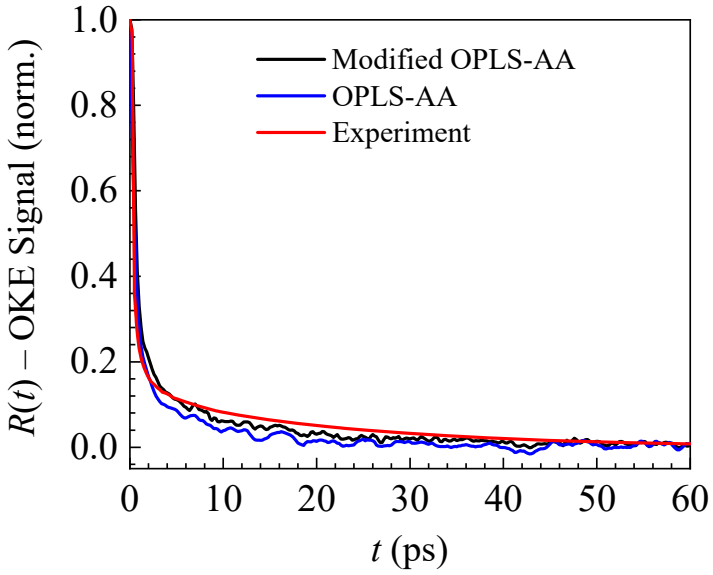


**Figure S3.** The simulated OKE signal of benzonitrile using the classic OPLS-AA force field (blue curve) and the modified OPLS-AA force field (black curve). The modified force field achieves slightly better agreement with the experimental OKE signal (red curve).

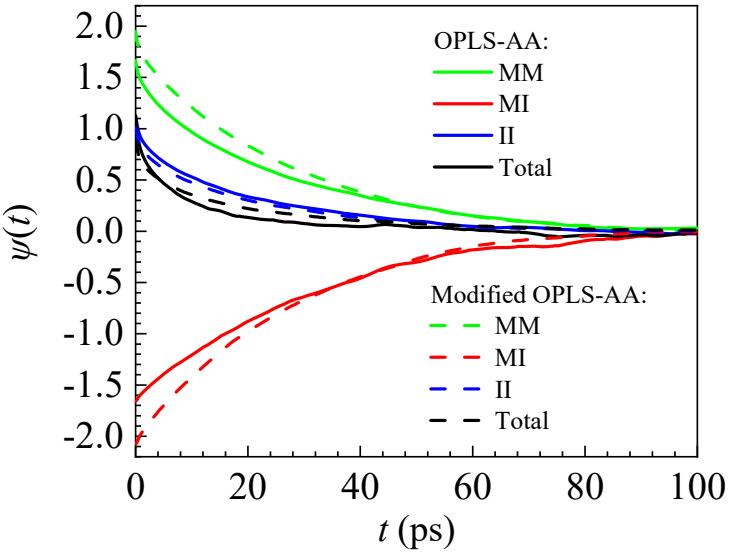


**Figure S4.** The PA-TCF of benzonitrile at 300 K using the classic OPLS-AA force field and modified OPLS-AA force field. The contributions of the molecular and interaction-induced autocorrelations and their cross-correlation are displayed for comparison to the PA-TCF.

### 3. The liquid structure factor of benzonitrile at 300 K

The liquid structure factor, $S(q)$, can be described by the following equation:

$$S(q) = \frac{\rho_0 \sum_i \sum_j x_i x_j f_i(q) f_j(q) \int_0^\infty 4\pi r^2 (g_{ij}(r) - 1) \frac{\sin qr}{qr} dr}{\left[\sum_i x_i f_i(q)\right]^2}. \quad \text{(S1)}$$

Here, $g_{ij}(r)$ corresponds to the partial radial pair distribution function (rdf) for atomic species of type *i* and type *j*. Specifically, the indices *i* and *j* span the set of constituent atoms that include C, H and N. $x_i$ and $x_j$ are the fractions of atoms of type *i* and *j*. $f_i$ and $f_j$ are the x-ray atomic form factors and $\rho_0$ is the total number density of the system. Using this equation in our MD simulation, we obtained the structure factor of benzonitrile and compared it to the experimental results from Katayama et al.[10] The simulation results agree well with the experiment, with only a slight difference in the peak height at 2.0 Å$^{-1}$, which corresponds to a 3.0-4.0 Å periodicity of benzonitrile. The good agreement demonstrates that our modified force field can reproduce the microstructure of liquid benzonitrile.

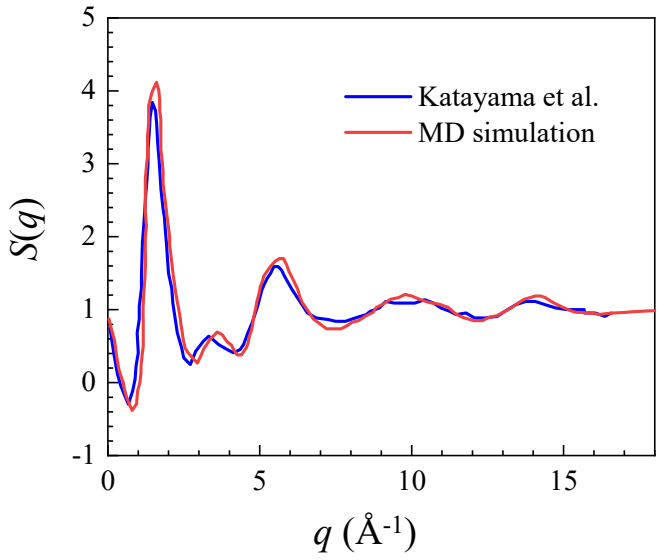


**Figure S5.** Liquid structure factor *S*(*q*) of benzonitrile using our modified OPLS-AA force field (red curve) and comparison to the experiment[10] (blue curve) at 300 K.

**4. Radial distribution function comparison between our modified OPLS-AA force field and other classic force fields**

A comparison of the mass center-mass center radial distribution function between our modified OPLS-AA force field and other classic force fields is shown in Fig. S6. The first intense peak and second peak locations remain almost unchanged with our modified force field and with the other force fields. The decrease in the first peak height using the Amber force field indicates that the order is lower and the structure is looser in the simulation. This, in part, explains why the simulated dynamical properties with the Amber force field are much faster compared to the values obtained with other force fields and experimentally.

Fig. S7 compares the N-H1 rdf between the simulations with different force fields. The N-H1 intermolecular interaction is a significant Coulombic interaction and a key driving force for the ordered antiparallel structure found in liquid benzonitrile (see main text). Interestingly, in this case the Charmm deviates the most from the other force fields in that the height of the most intense peak is comparatively lower.

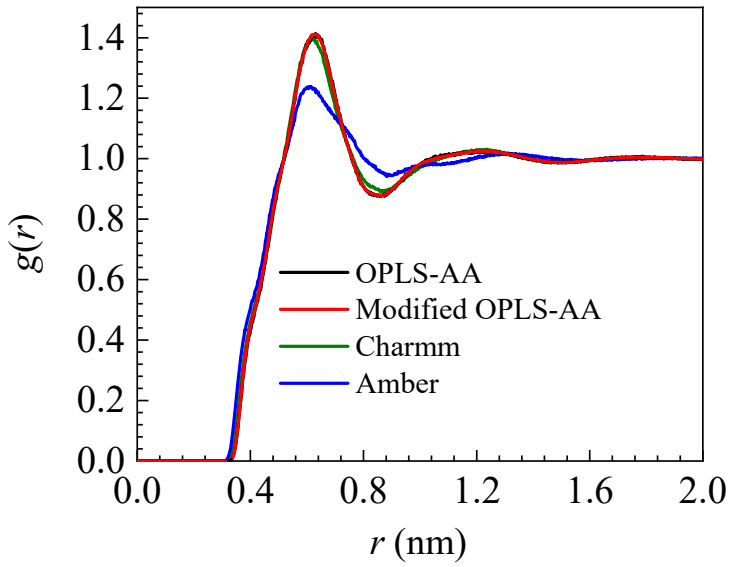


**Figure S6.** Comparison between the mass center-mass center radial distribution function for our modified OPLS-AA force field and other classic force fields at 300 K.

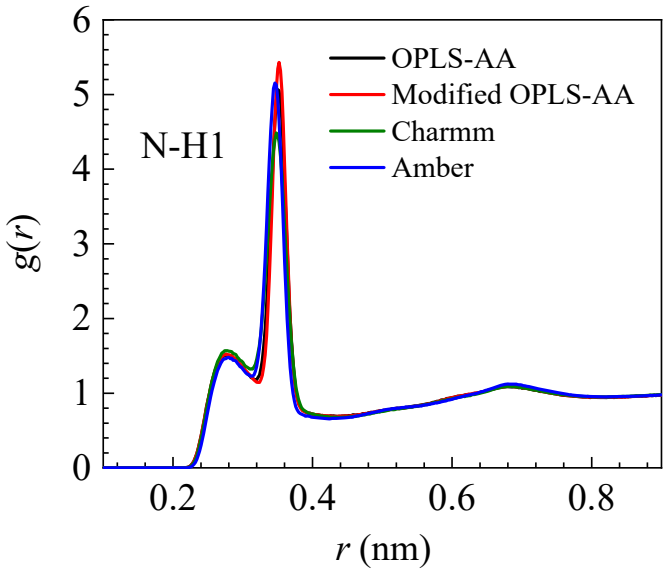


**Figure S7.** Comparison between the N-H1 site-site radial distribution function for our modified OPLS-AA force field and other classic force fields at 300 K.

**5. Temperature-dependent self-diffusion coefficients**

The temperature-dependent self-diffusion coefficients for benzonitrile calculated with our modified OPLS-AA force field are shown in Fig. S8. The temperature-dependent translational diffusion dynamics of benzonitrile follow a classic Arrhenius behavior. The fit equation is $D = D_0 \exp(-E_a / k_B T)$, where $D_0 = 342.22 \times 10^{-5}$ cm$^2$s$^{-1}$ and the activation energy is $E_a = 4.56$ kJ/mol.

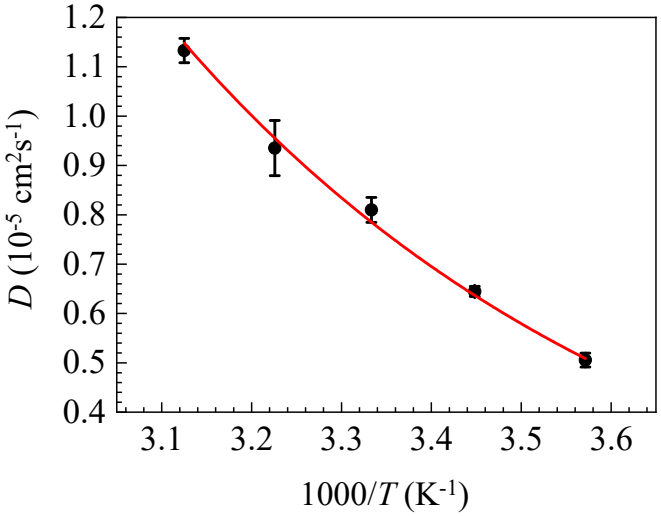


**Figure S8.** The calculated temperature-dependent self-diffusion coefficients for our modified OPLS-AA force field (black points). The red curve is the fit.

## 6. Semi-log plot of the simulated and experimental OKE signal

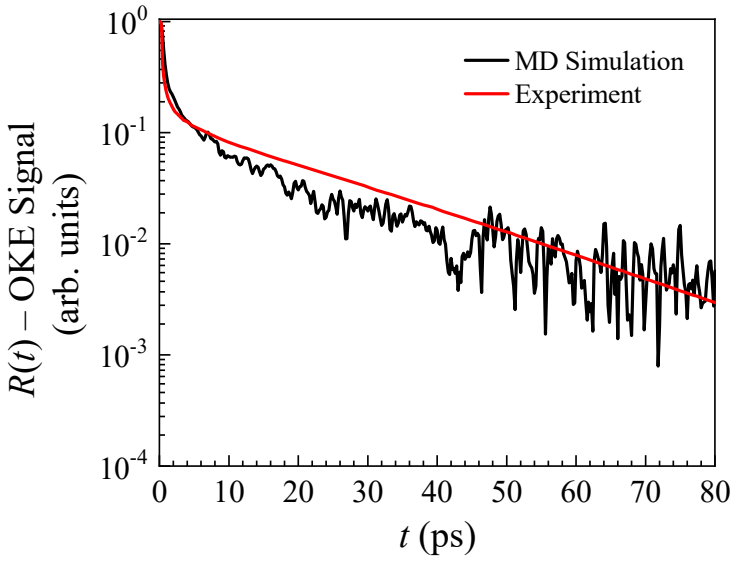


**Figure S9.** Comparison between the simulated (black curve) and experimental (red curve) OKE signal on a semi-log plot.

## 7. Single-exponential fit to the simulated OKE signal decay

The OKE signal can be obtained by differentiating the polarizability anisotropy time correlation function (TCF), $\psi(t)$, according to Eq. (19). We again note that because bulk benzonitrile is macroscopically isotropic, we can average together all anisotropic components of the collective polarizability tensor when calculating $\psi(t)$. The polarizability anisotropy TCF in Fig. 5 of the main text appears well-averaged and smooth. However, performing the numerical time-differentiation of $\psi(t)$ introduces noise and leads to additional roughness in the decay curve particularly at long time. This can be seen in Fig. S10, which magnifies the 20 to 80 ps region of the decay. Previous OKE simulation studies have taken an alternative approach by first fitting an exponential function to $\psi(t)$ and then differentiating this exponential fit to obtain the final OKE decay, $R(t)$.[11] Here, we directly differentiated the TCF to obtain $R(t)$, which agrees well with the experimental data over the entire relaxation process time range (see Fig. 4).

The collective polarizability anisotropy TCF can be described by a series of power laws preceding a single exponential using Mode Coupling Theory.[12] The current work focuses solely on the exponential region. The long-time portion of the simulated $R(t)$ can be fit with a single-

exponential of the form $R(t) = A\exp[-t/\tau_c]$. The fit parameters with standard errors are $A$ = 0.0553 ± 0.003, $\tau_c$ = 28.8 ± 1.1 ps.

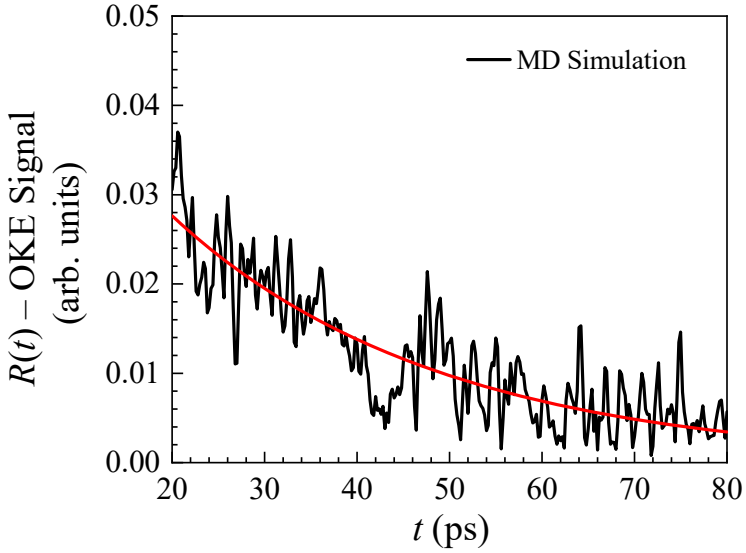


**Figure S10.** Single-exponential fit (red curve) to the simulated OKE signal (black curve) from 20 to 80 ps.

**8. Plot of the second-order Legendre polynomial**

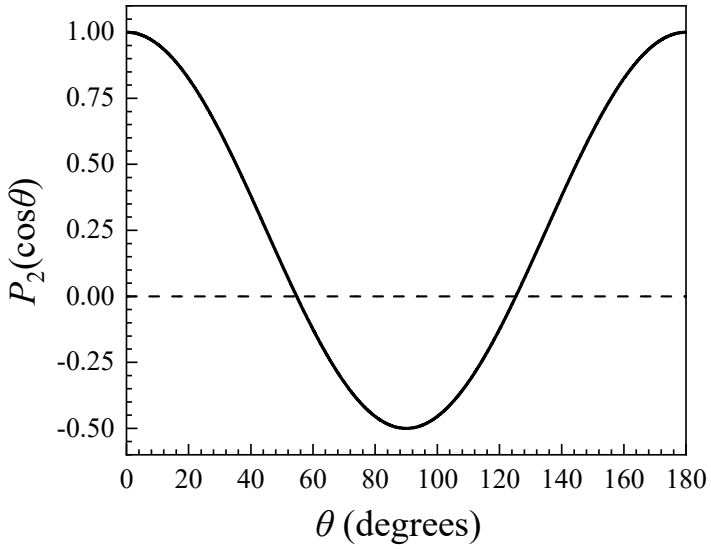


**Figure S11.** The second-order Legendre polynomial, $P_2(\cos\theta)$, versus $\theta$.

**9. Single-exponential fit to the simulated $C_2(t)$ for the benzonitrile CN bond unit vector**

The anisotropy, $r(t)$, or equivalently the second order Legendre polynomial orientational correlation function, $C_2(t) = 2.5r(t)$, tracks the single molecule reorientational dynamics of the benzonitrile CN bond unit vector. The decay at long time is dominated by free diffusion and can be described well by a single-exponential. This same fitting approach was taken in a previous work.[13] As discussed in the main text, the long-time decay should be biexponential according to the theory originally outlined by Favro.[14] However, the amplitude of one exponential is predicted to be very small such that it is difficult to detect. Using a single exponential fit of the form, $C_2(t) = A\exp[-t/\tau_s]$, over the range from 20 to 80 ps, the resulting fit parameters with standard errors are $A = 0.617 \pm 0.003$ and $\tau_s = 17.2 \pm 0.1$ ps.

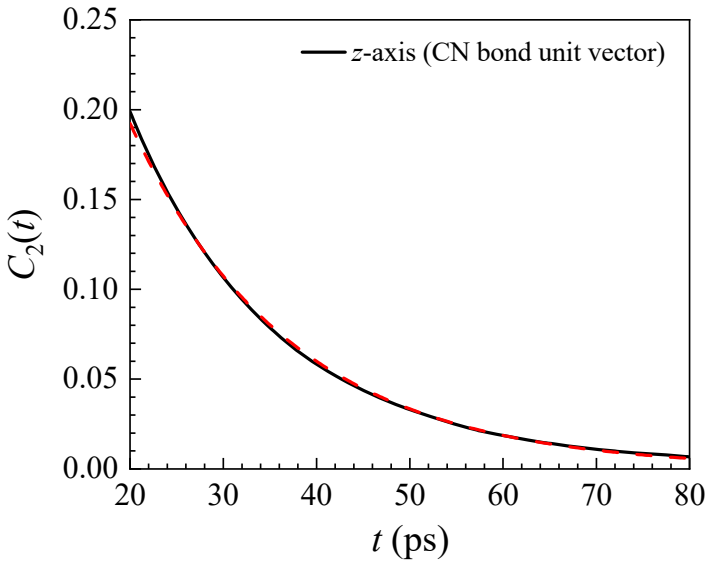


**Figure S12.** Single-exponential fit (dashed red curve) to the simulated $C_2(t)$ for the CN bond unit vector, or z-axis direction (black curve).

## 10. Comparison of $\psi^{MM,s}(t)$ and $C_2(t)$

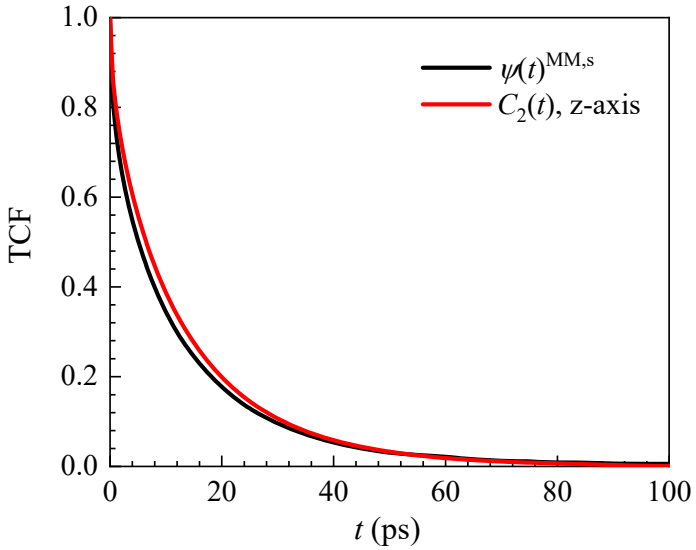


**Figure S13.** Comparison of $\psi^{MM,s}(t)$ (black curve) and $C_2(t)$ for the C-N bond unit vector of benzonitrile (red curve).

## 11. Velocity autocorrelation function

The translational velocity autocorrelation function for benzonitrile is shown in Fig. S14. One of the distinctive features of the correlation function is a negative region that occurs after several hundred femtoseconds. A low amplitude recurrence is also evident. It has been suggested that the negative region becomes more pronounced in high density liquids.[15] This region is interpreted as arising from the reversal of the velocity of the molecule after interacting with its first solvent shell of molecules and is a reflection of so-called "caging" dynamics. It is important to note that if the time-sequence of the interactions between the molecule with its surroundings is a Gaussian Markov process, the correlation function is a single exponential decay, and no such negative region exists.[15]

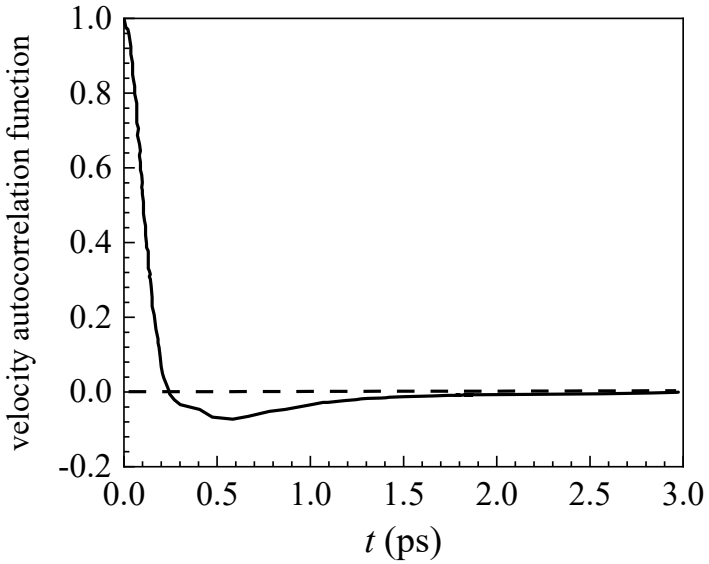


**Figure S14.** The simulated translational velocity autocorrelation function for benzonitrile.

**12. Rotational mean squared displacement calculation**

To calculate $D_r$, we consider the behavior of a random unit vector $\vec{u}_i(t)$ for molecule *i*. Molecular rotation will change the orientation of the vector. Naïvely, one may define angular displacement as $\vec{u}_i(t) - \vec{u}_i(0)$. The problem with this definition is that it results in a bounded quantity and does not provide a complete picture of the full extent of molecular reorientation. Following the approach of Mazza et al.,[16] we avoid this complication by defining the vector rotational displacement in the time interval $[t, t+\Delta t]$ as $\vec{\phi}_i(\Delta t) \equiv \int_t^{t+\Delta t} \Delta\vec{\phi}_i(t')\mathrm{d}t'$, where $\Delta\vec{\phi}_i(t')$ is a vector with direction given by $\vec{u}_i(t') \times \vec{u}_i(t'+\mathrm{d}t')$ and with magnitude given by $\left|\Delta\vec{\phi}_i(t')\right| \equiv \cos^{-1}[\vec{u}_i(t') \cdot \vec{u}_i(t'+\mathrm{d}t')]$. We define, in analogy to the mean squared displacement, a rotational mean squared displacement (RMSD), $\langle\phi^2(\Delta t)\rangle \equiv \frac{1}{N}\sum_{i=0}^{N} |\vec{\phi}_i(t+\Delta t) - \vec{\phi}_i(t)|^2$. Using this form, we define $D_r$ as $D_r \equiv \lim_{\Delta t\to\infty} \frac{1}{4\Delta t}\langle\phi^2(\Delta t)\rangle$.

**References**


1. Lemkul, J., From proteins to perturbed Hamiltonians: A suite of tutorials for the GROMACS-2018 molecular simulation package [article v1. 0]. *Living J. Comp. Mol. Sci.* **2018,** *1*, 5068.

2. Jorgensen, W. L.; Laird, E. R.; Nguyen, T. B.; Tirado-Rives, J., Monte Carlo simulations of pure liquid substituted benzenes with OPLS potential functions. *J. Comput. Chem.* **1993,** *14* (2), 206-215.

3. Wang, J.; Wolf, R. M.; Caldwell, J. W.; Kollman, P. A.; Case, D. A., Development and testing of a general amber force field. *J. Comput. Chem.* **2004,** *25* (9), 1157-1174.

4. Vanommeslaeghe, K.; Hatcher, E.; Acharya, C.; Kundu, S.; Zhong, S.; Shim, J.; Darian, E.; Guvench, O.; Lopes, P.; Vorobyov, I.; Mackerell Jr., A. D., CHARMM general force field: A force field for drug-like molecules compatible with the CHARMM all-atom additive biological force fields. *J. Comput. Chem.* **2010,** *31* (4), 671-690.

5. Falcone, D. R.; Douglass, D. C.; McCall, D. W., Self-diffusion in benzene. *J. Phys. Chem.* **1967,** *71* (8), 2754-2755.

6. Polzin, B.; Weiss, A., Transport Properties of Liquids. VIII. Molar Volume and Selfdiffusion of Organic Liquids at Pressures up to 200 MPa. *Berichte der Bunsengesellschaft für physikalische Chemie* **1990,** *94* (7), 746-758.

7. Viswanathan, S.; Anand Rao, M.; Prasad, D. H. L., Densities and Viscosities of Binary Liquid Mixtures of Anisole or Methyl tert-Butyl Ether with Benzene, Chlorobenzene, Benzonitrile, and Nitrobenzene. *J. Chem. & Eng. Data* **2000,** *45* (5), 764-770.

8. Nikam, P. S.; Kharat, S. J., Excess Molar Volumes and Deviations in Viscosity of Binary Mixtures of N,N-Dimethylformamide with Aniline and Benzonitrile at (298.15, 303.15, 308.15, and 313.15) K. *J. Chem. & Eng. Data* **2003,** *48* (4), 972-976.

9. Frisch, M. J.; Trucks, G. W.; Schlegel, H. B.; Scuseria, G. E.; Robb, M. A.; Cheeseman, J. R.; Montgomery, J., J. A.; Vreven, T.; Kudin, K. N.; Burant, J. C.; Millam, J. M.; Iyengar, S. S.; Tomasi, J.; Barone, V.; Mennucci, B.; Cossi, M.; Scalmani, G.; Rega, N.; Petersson, G. A.; Nakatsuji, H.; Hada, M.; Ehara, M.; Toyota, K.; Fukuda, R.; Hasegawa, J.; Ishida, M.; Nakajima, T.; Honda, Y.; Kitao, O.; Nakai, H.; Klene, M.; Li, X.; Knox, J. E.; Hratchian, H. P.; Cross, J. B.; Bakken, V.; Adamo, C.; Jaramillo, J.; Gomperts, R.; Stratmann, R. E.; Yazyev, O.; Austin, A. J.; Cammi, R.; Pomelli, C.; Ochterski, J. W.; Ayala, P. Y.; Morokuma, K.; Voth, G. A.; Salvador,

P.; Dannenberg, J. J.; Zakrzewski, V. G.; Dapprich, S.; Daniels, A. D.; Strain, M. C.; Farkas, O.; Malick, D. K.; Rabuck, A. D.; Raghavachari, K.; Foresman, J. B.; Ortiz, J. V.; Cui, Q.; Baboul, A. G.; Clifford, S.; Cioslowski, J.; Stefanov, B. B.; Liu, G.; Liashenko, A.; Piskorz, P.; Komaromi, I.; Martin, R. L.; Fox, D. J.; Keith, T.; Al-Laham, M. A.; Peng, C. Y.; Nanayakkara, A.; Challacombe, M.; Gill, P. M. W.; Johnson, B.; Chen, W.; Wong, M. W.; Gonzalez, C.; and Pople, J. A., Gaussian 03, Revision C. 02. Gaussian Inc. Wallingford, CT, 2004.

10. Katayama, M.; Komori, K.; Ozutsumi, K.; Ohtaki, H., The Liquid Structure of Various Nitriles and N,N-Dimethylformamide Studied by the X-Ray Diffraction Method Using a CCD Detector. *Z. Phys. Chem.* **2004,** *218* (6), 659.

11. Milischuk, A. A.; Ladanyi, B. M., Polarizability Anisotropy Relaxation in Nanoconfinement: Molecular Simulation Study of Acetonitrile in Silica Pores. *J. Phys. Chem. B* **2013,** *117* (49), 15729-15740.

12. Götze, W.; Sjögren, L., The mode coupling theory of structural relaxations. *Transport Theory and Stat. Phys.* **1995,** *24* (6-8), 801-853.

13. Yamada, S. A.; Bailey, H. E.; Fayer, M. D., Orientational Pair Correlations in a Dipolar Molecular Liquid: Time-Resolved Resonant and Nonresonant Pump–Probe Spectroscopies. *J. Phys. Chem. B* **2018,** *122* (50), 12147-12153.

14. Favro, L. D., Theory of the Rotational Brownian Motion of a Free Rigid Body. *Phys. Rev.* **1960,** *119* (1), 53-62.

15. Berne, B. J.; Boon, J. P.; Rice, S. A., On the Calculation of Autocorrelation Functions of Dynamical Variables. *J. Chem. Phys.* **1966,** *45* (4), 1086-1096.

16. Mazza, M. G.; Giovambattista, N.; Stanley, H. E.; Starr, F. W., Connection of translational and rotational dynamical heterogeneities with the breakdown of the Stokes-Einstein and Stokes-Einstein-Debye relations in water. *Phys.l Rev. E* **2007,** *76* (3), 031203.